Broadband and Miniaturized Antenna-in-Package (AiP) Design for 5G Applications

Tong-Hong Lin, *Student Member, IEEE*, Kimiyuki Kanno, Atom O. Watanabe, *Student Member, IEEE*, Pulugurtha Markondeya Raj, Rao R. Tummala, *Life Fellow, IEEE*, Madhavan Swaminathan, *Fellow, IEEE*, and Manos M. Tentzeris, *Fellow, IEEE*

Abstract—A broadband and miniaturized planar Yagi antenna-in-package (AiP) design for the fifth-generation (5G) wireless communication is proposed. The monopole taper radiator is adopted for the proposed Yagi antenna design to miniaturize the size, extend the bandwidth, and simplify the feeding network. The proposed AiP design is broadband enough to cover all three 5G New Radio bands simultaneously. The high-precision high-resolution multilayered glass packaging fabrication process with a new low-loss polymer material coating is adopted to realize the circuit. The operation band is from 24.25 to 40 GHz and the fractional bandwidth is 49%. The overall size for an antenna element is 3.05 mm × 5.56 mm, which is equal to $0.25 \lambda_0 \times 0.45 \lambda_0$. The measured S_{11} is smaller than -10 dB within the entire band and the gain is larger than 4 dBi. A two-by-one array using the proposed element is also demonstrated with a gain higher than 6.2 dBi within the entire band. Compared with previous works, the proposed AiP design can cover all 5G bands with a competitive size. Thus, it is suitable to be applied to massive arrays and easily integrated into packages to achieve compact system-in-package applications while resolving numerous current 5G challenges, including millimeter-wave (mm-wave) path loss and transmission loss.

Index Terms—Antenna array, antenna-in-package (AiP), broadband, fifth generation (5G), glass packaging, millimeter-wave (mm-wave), miniaturized.

I. INTRODUCTION

NUMEROUS opportunities and challenges have emerged with the launching of the new 5G wireless communication [1]. The adoption of millimeter-wave (mm-wave) frequencies and a wider spectrum provide the 5G communication a much higher data rate, low end-to-end latency, and the ability to connect more users simultaneously. These advantages are

Tong-Hong Lin, Atom O. Watanabe, Rao R. Tummala, Madhavan Swaminathan, and Manos M. Tentzeris are with the School of Electrical and Computer Engineering, Georgia Institute of Technology, Atlanta, GA 30332-250 USA (e-mail: colinjet2003@gmail.com; atom@gatech.edu; rao.tummala@ece.gatech.edu; madhavan.swaminathan@ece.gatech.edu; etentze@ece.gatech.edu).

Kimiyuki Kanno is with the JSR Corporation, Mie, 510-0871, Japan (e-mail: Kimiyuki_Kanno@jsr.co.jp).

Pulugurtha Markondeya Raj is with the Department of Biomedical Engineering, Florida International University, Miami, FL 33174 USA (e-mail: mpulugur@fiu.edu).
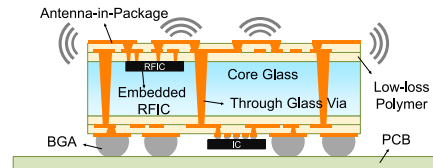
Fig. 1. Three-dimensional SiP module with AiP designs for 5G applications.

used to advance the development of emerging technologies, including automatic driving and Internet of Things. However, the high over-the-air path loss and high transmission loss within the circuit board at mm-wave range remain great challenges.

The mm-wave beamforming technology has been a popular method to solve the high over-the-air path loss problem [2], [3]. In the meantime, antenna-in-package (AiP) technology remains an attractive solution to reduce the high transmission loss at mm-wave range [2], [4], [5]. The schematic of a 3-D system-in-package (SiP) module with AiP designs for 5G applications is shown in Fig. 1. The mm-wave radio frequency integrated circuit (RFIC) is embedded inside a cavity and placed at the proximity of the AiP designs while other low-frequency ICs can be flip-chip bonded at longer distances. Since the originally on-board antenna arrays are now migrating to AiP designs, the interconnect lengths and the resulting transmission losses between RFIC and antennas are significantly reduced.

Taking both beamforming and AiP into consideration, massive arrays that can enhance the gain values and beamforming capabilities while the overall sizes are small enough to be integrated inside the package are necessary. Current 5G New Radio (NR) standard utilize three different bands: n257 (26.5–29.5 GHz), n258 (24.25–27.5 GHz), and n260 (37–40 GHz). If three sets of antenna arrays covering each band have to be integrated into a single package, the element number in each array has to be reduced resulting in the decrease of the gain values and beamforming capabilities. Thus, a broadband and miniaturized AiP element design, which covers all three bands from 24.25 to 40 GHz, is necessary to reduce the set of arrays and achieve better performances. Recently there have been many reports of AiP element designs and research works using different fabrication processes. In [6], a 3-D printed AiP is introduced. A multilayer AiP structure utilizing organic substrates has been described in [2]. However, these designs are not broadband enough to cover the whole 5G band and the sizes can be further improved.

Fig. 2.   Stack-up for the proposed broadband and miniaturized AiP design.

Fig. 3.   Geometry of the proposed broadband and miniaturized AiP element design.

Fig. 4.   Geometry of the two-by-one AiP array design.

In this letter, a broadband planar Yagi–Uda AiP element is proposed to cover all three 5G bands from 24.25 to 40 GHz. To miniaturize the size, the antenna element structure is modified to simplify the feeding network while removing the requirement for the balun. For the Yagi element design, instead of the dipole-type radiator, the monopole-type radiator is used to further reduce the size. Both a single antenna element and a two-by-one array are demonstrated. The low-cost good-scalability glass packaging technology [7]–[9], which offers great surface roughness, coefficient of thermal expansion match to silicon dies, and fine-pitch lines, spaces [10], and vias [11] for high-speed high-I/O computation, is adopted for the fabrication. Broadband characteristics and excellent endfire radiation capability are confirmed with the measured return losses, gain values, and radiation patterns.

II. ANTENNA ELEMENT AND ARRAY DESIGN

A. Glass Packaging Stack-Up

The stack-up for the proposed broadband and miniaturized AiP design is shown in Fig. 2. The material and the thickness of each layer are also included. The core substrate is a 100 μm EN-A1 glass from Asahi Glass Company (AGC). The dielectric constant is 5.41 and the loss tangent is 0.006 at 35 GHz. Two 15 μm layers of low-loss polymer developed by JSR Corporation are coated on the top of the glass to reduce the overall loss tangent. This new-developed material has large elongation factor and is softer, which can be used to effectively prevent warpage in multilayer packaging realization and is applied to the glass packaging process for the first time. Measuring at 32 GHz, the dielectric constant and loss tangent for this low-loss polymer are 2.8 and 0.0045 [12], respectively. Two layers of metal denoted by M1 and M2 are realized with copper. Finally, a 30 μm layer of polymer is coated on the bottom of the glass to balance the weight and prevent the warpage.

B. Element and Array Design

The geometry of the proposed broadband and miniaturized AiP element design is demonstrated in Fig. 3. The physical dimensions in millimeters are: CPW_w = 0.62, CPW_ gap = 0.06, rad_w1 = 2.8, rad_w2 = 2.29, ref_gap1 = 1.2, ref_gap2 = 0.78, dir_l = 2.2, dir_gap = 0.12, dir_w = 0.4, ant_w = 5.56, and ant_l = 3.05. All structures are realized only at metal layer M1 shown in Fig. 2. The other metal layer M2 is only used in the array design. As shown in Fig. 3, compared with the conventional quasi-Yagi antenna, which utilized dipole as the radiator [13], the proposed antenna element used monopole as
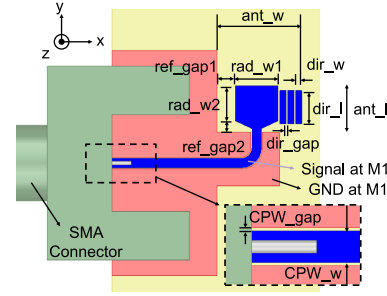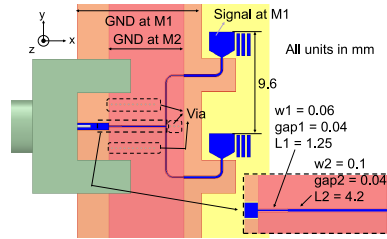
the radiator featuring two major advantages. One is the reduction of size by half and the other is the removal of the requirement of the differential feeding or the balun, which can further reduce the size and simplify the feeding network design. Thus, a simple coplanar waveguide (CPW) can be used as the feeding network and alleviate the difficulties in broadband feeding network design. A 90° bend on the radiator is introduced so that the ground plane of the CPW can be directly used as the reflector for the Yagi antenna and the layout for the antenna array can be simplified. The square radiator with a tapered shaped near the feeding point is used to broaden the operational bandwidth.

The structure of the two-by-one array design is shown in Fig. 4. The interelement spacing is 9.6 mm. Additional ground planes at the M2 layer and via arrays connecting M1 and M2 with 235 μm pitches and 35 μm diameters are used to ensure that all ground planes are connected together. A two-stage quarter-wave transformer is used for impedance matching at the feeding network and the respective CPW widths, gaps, and lengths are shown in Fig. 4.

III. FABRICATION PROCESS

The semiadditive patterning (SAP) process was employed for the fabrication of broadband and miniaturized Yagi antenna. SAP enables precise patterning and fine features, such as sub-5 μm copper traces because of dimensional stability and surface planarity of the glass panel and the capability to accurately control the thickness of the dielectric that is spin-coated onto the glass core. The whole process with side-view images is illustrated in Fig. 5. The glass panels are treated with silane to promote adhesion between dielectric and them and prevent delamination during the whole fabrication process. The dielectric is spin-coated on both sides of the glass panel and cured. Thin titanium, which acted as a barrier to prevent copper
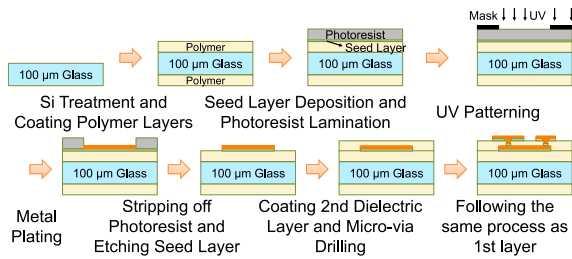
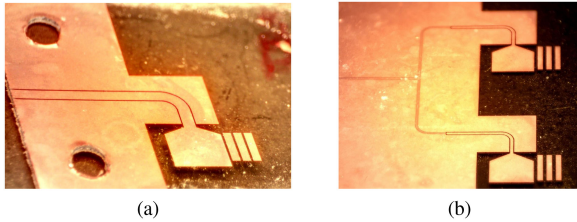Fig. 5.   Fabrication process of the AiP glass packaging technology.

Fig. 6.   Prototypes of the proposed broadband and miniaturized Yagi AiP. (a) Element design. (b) Array design.

from migrating into the substrate, and the copper seed layer are deposited with the sputtering process after dry etching, which cleans the surface of the dielectric. Although the electroless plating provides an anchor effect with a rough surface and, thus, high adhesion strength between the seed layer and dielectric, the combination of the sputtered seed layer and the optimized liquid dielectric also lead to high adhesion strength mitigating surface roughness and conductive loss [12]. Next, the panel is laminated with a dry-film negative photoresist. The panel with photoresist is patterned with optimized ultraviolet (UV) dose time. Then, the panel is treated with oxygen plasma to remove the photoresist beneath the pattern for copper plating. The metal patterning for M2 is performed through the SAP process with a controlled metal thickness of 5–8 μm.

Afterward, the second dielectric layer is spin-coated following the same process as the first layer. Microvias were formed using a UV laser tool. The laser condition, such as power density and the number of repetitions, is optimized to drill 35 μm vias in the dielectric. After the microvia formation, dry desmear is used to clean the surface and remove residual polymer, followed by seed layer deposition sequentially. Finally, the metal patterning for M1 is performed again through the SAP process. The same process can be used to pattern metal on both sides of the glass if needed.

IV. EXPERIMENTAL RESULTS AND ANALYSIS

A. Antenna Element

The fabricated proof-of-concept prototype of the proposed broadband and miniaturized Yagi AiP element is shown in Fig. 6(a) and the measured S_{11} as well as gain are shown in Fig. 7. The full-wave simulated results are obtained using Ansys HFSS. Since at mm-wave range, the parasitics and effects of the subminiature version A (SMA) connector cannot be ignored, the module of the SMA connector is also included in simulation for
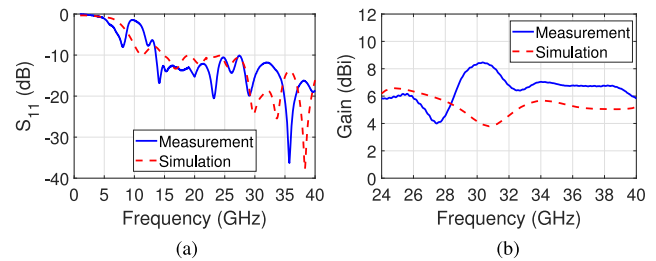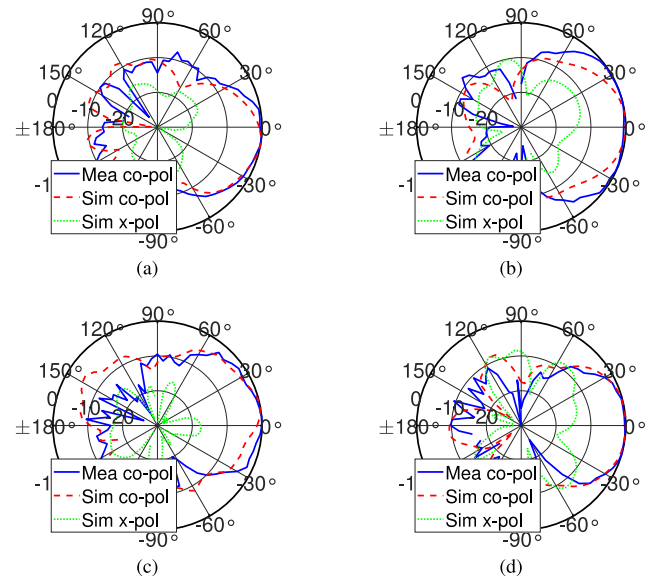

Fig. 7.   Measured and simulated (a) S_{11} and (b) gain of the proposed broadband and miniaturized Yagi AiP element design.

Fig. 8.   Measured and simulated normalized radiation patterns for Yagi AiP element design at (a) 24.25 GHz E-plane, (b) 24.25 GHz H-plane, (c) 40 GHz E-plane, and (d) 40 GHz H-plane.

codesign, as shown in Fig. 3. As shown in Fig. 7(a), the measured S_{11} is lower than -10 dB from 13.58 to 40 GHz. Thus, the three 5G bands from 24.25 to 40 GHz are fully covered. Moreover, as shown in Fig. 7(b), the measured gain is higher than 4 dBi within the entire 5G bands. The measured gains are slightly higher than the simulated ones since when simulating the designs, the loss tangent values of the core glass and JSR polymer are set to the largest values within the band rather than frequency dependent to obtain the lower bound results.

The measured and simulated normalized radiation patterns are lowest at 24.25 GHz and highest at 40 GHz operating frequencies as shown in Fig. 8. Besides, both E-plane and H-plane patterns are included. The 0° direction is the endfire, positive *x* in Fig. 3, direction. Although the main-beam directions are not always at 0°, they are very close to it within the entire operating band. The simulated cross-polarization results are also included and are less than -15 dB at main-beam directions.

B. Antenna Array

The fabricated prototype of two-by-one Yagi array is shown in Fig. 6(b), whereas the measured and simulated S_{11} and gain are demonstrated in Fig. 9. The measured S_{11} is lower than -9 dB

TABLE I
COMPARISON BETWEEN THIS WORK AND PREVIOUS RELATED WORKS

| Work	Technique	Operating Frequency (GHz)	FBW (%)	Gain (dBi)	Size (λ_0)	Pattern	Antenna
[14]	PCB	24.5 - 31.72	25.7	7.2	0.82×1.98	End-fire	SIW dipole
[15]	PCB	26.5 - 38.2	36.2	4.5	0.34×0.35	End-fire	Angled dipole
[16]	AiP from active module	28 - 29.6	5.6	4.0	0.22×0.22	Broadside	Patch
[17]	AiP from active module	26.7 - 30	11.6	4.0	0.6×0.6	Broadside	Patch
[18]	AiP from active module	28 - 32	13.3	4.5	0.48×0.57	Broadside	Patch
[2]	Organic AiP	30 - 30.8	2.6	4.9	0.6×0.6	Broadside	Patch
[6]	3D printing AiP	22.4 - 30.1	29.3	5.0	0.28×0.64	End-fire	Yagi
This work	Glass AiP	24.25 - 40	49.0	4.0	0.25×0.45	End-fire	Yagi
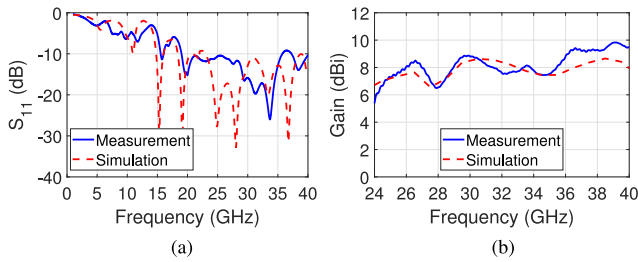
Fig. 9. Measured and simulated (a) S_{11} and (b) gain of the proposed broadband and miniaturized Yagi two-by-one array design.
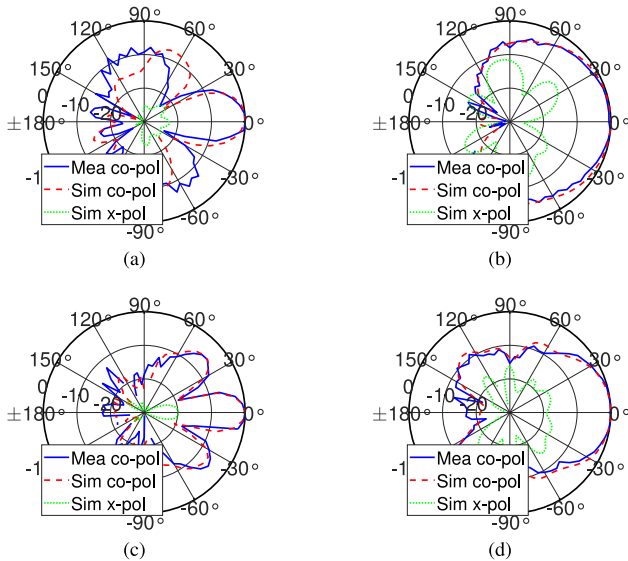

Fig. 10. Measured and simulated normalized radiation patterns for Yagi AiP two-by-one array design at (a) 24.25 GHz E-plane, (b) 24.25 GHz H-plane, (c) 40 GHz E-plane, and (d) 40 GHz H-plane.

from 18.87 to 40 GHz. The minor degradation compared to the single element design is due to the insertion of the two-stage quarter-wave transformer at the feeding network for matching. However, good performances within the entire 5G bands can be observed. The measured gain is higher than 6.2 dBi within the entire band.

The measured normalized radiation patterns at the 24.25 and 40 GHz operating frequencies are shown in Fig. 10. The simulated results are also included for comparison and a good

agreement can be observed. The grating lobes in Fig. 10(c) are because of the relatively long element separation distance at 40 GHz and can be improved by reducing the separation distance. The simulated cross-polarization results are also included and they are all lower than −19 dB in the main-beam direction. The main-beam beamwidths at E-plane are narrower than the respective H-plane results. The reason is that the array is arranged alone y-direction, as shown in Fig. 4.

C. Comparison

The comparisons between the proposed work and previous work are summarized in Table I. All parameters are based on a single antenna element. Numerous designs operating at 5G frequency bands using either printed circuit board (PCB) or AiP topologies are included for comparison. λ_0 in the size is the wavelength at the lowest operating frequency. The simple transmission line parts of the feeding networks are excluded while calculating the sizes. As shown in Table I, the proposed work achieves the largest fractional bandwidth (FBW) and is the only one that can fully cover all three 5G NR operating bands. Moreover, the size of the proposed works is smaller than all other works except the one in [16]. Although the proposed work is about 2.3 times larger than it, the proposed work can offer 8.75 times larger bandwidth compared with it.

V. CONCLUSION

This letter reports the first broadband and miniaturized planar Yagi AiP design, which can cover all three major 5G NR operating bands from 24.25 to 40 GHz simultaneously while maintaining a small form factor. The FBW is 49% and the size for the antenna element is 3.05 mm × 5.56 mm, which equals 0.25 λ_0 × 0.45 λ_0 where λ_0 is the wavelength at 24.25 GHz. Both the single element and the two-by-one array design are simulated, fabricated, and measured. The glass multilayered packaging with a new polymer material is used to realize the designs. The element gain is higher than 4 dBi and the array gain is higher than 6.2 dBi within the entire operating band. The normalized radiation patterns at E-plane and H-plane are demonstrated and the main-beam directions are consistent within the entire band. The cross-polarized patterns at the main-beam direction are smaller than −15 dB. The comparison between this letter and prior works is summarized. This letter demonstrates the largest bandwidth with a comparable size.

REFERENCES

[1] J. Thompson *et al.*, "5G wireless communication systems: Prospects and challenges [Guest Editorial]," *IEEE Commun. Mag.*, vol. 52, no. 2, pp. 62–64, Feb. 2014.

[2] D. Liu, X. Gu, C. W. Baks, and A. Valdes-Garcia, "Antenna-in-package design considerations for Ka-band 5G communication applications," *IEEE Trans. Antennas Propag.*, vol. 65, no. 12, pp. 6372–6379, Dec. 2017.

[3] W. Roh *et al.*, "Millimeter-wave beamforming as an enabling technology for 5G cellular communications: Theoretical feasibility and prototype results," *IEEE Commun. Mag.*, vol. 52, no. 2, pp. 106–113, Feb. 2014.

[4] Y. Lu, B. Fang, H. Mi, and K. Chen, "Mm-wave antenna in package (AiP) design applied to 5th generation (5G) cellular user equipment using unbalanced substrate," in *Proc. IEEE 68th Electron. Compon. Technol. Conf.*, 2018, pp. 208–213.

[5] T. Lin, R. A. Bahr, and M. M. Tentzeris, *Additive Manufacturing AiP Designs and Applications*. Hoboken, NJ, USA: Wiley, 2020, Ch. 9, pp. 267–291. [Online]. Available: https://onlinelibrary.wiley.com/doi/abs/10.1002/9781119556671.ch9

[6] T. Lin, R. Bahr, M. M. Tentzeris, P. M. Raj, V. Sundaram, and R. Tummala, "Novel 3D-/inkjet-printed flexible on-package antennas, packaging structures, and modules for broadband 5G applications," in *Proc. IEEE 68th Electron. Compon. Technol. Conf.*, 2018, pp. 214–220.

[7] T. Lin, P. M. Raj, A. Watanabe, V. Sundaram, R. Tummala, and M. M. Tentzeris, "Nanostructured miniaturized artificial magnetic conductors (AMC) for high-performance antennas in 5G, IoT, and smart skin applications," in *Proc. IEEE 17th Int. Conf. Nanotechnol.*, 2017, pp. 911–915.

[8] A. O. Watanabe *et al.*, "First demonstration of 28 GHz and 39 GHz transmission lines and antennas on glass substrates for 5G modules," in *Proc. IEEE 67th Electron. Compon. Technol. Conf.*, 2017, pp. 236–241.

[9] C. Buch *et al.*, "Design and demonstration of highly miniaturized, low cost panel level glass package for MEMS sensors," in *Proc. IEEE 67th Electron. Compon. Conf.*, 2017, pp. 1088–1097.

[10] F. Liu *et al.*, "Via-in-trench: A revolutionary panel-based package RDL configuration capable of 200-450 IO/mm/layer, an innovation for more-than-Moore system integration," in *Proc. IEEE 67th Electron. Compon. Technol. Conf.*, 2017, pp. 2097–2103.

[11] S. Viswanathan *et al.*, "High frequency electrical performance and thermo-mechanical reliability of fine-pitch, copper-metallized through-package-vias (TPVs) in ultra-thin glass interposers," in *Proc. IEEE 67th Electron. Compon. Technol. Conf.*, 2017, pp. 1510–1516.

[12] H. Ito *et al.*, "Advanced low-loss and high-density photosensitive dielectric material for RF/millimeter-wave applications," in *Proc. Int. Wafer Level Packag. Conf.*, 2019, pp. 1–6.

[13] N. Kaneda, W. R. Deal, Y. Qian, R. Waterhouse, and T. Itoh, "A broadband planar quasi-Yagi antenna," *IEEE Trans. Antennas Propag.*, vol. 50, no. 8, pp. 1158–1160, Aug. 2002.

[14] W. El-Halwagy, R. Mirzavand, J. Melzer, M. Hossain, and P. Mousavi, "Investigation of wideband substrate-integrated vertically-polarized electric dipole antenna and arrays for mm-wave 5G mobile devices," *IEEE Access*, vol. 6, pp. 2145–2157, 2018.

[15] S. X. Ta, H. Choo, and I. Park, "Broadband printed-dipole antenna and its arrays for 5G applications," *IEEE Antennas Wireless Propag. Lett.*, vol. 16, pp. 2183–2186, 2017.

[16] H. Kim *et al.*, "A 28GHz CMOS direct conversion transceiver with packaged antenna arrays for 5G cellular system," in *Proc. IEEE Radio Freq. Integr. Circuits Symp.*, 2017, pp. 69–72.

[17] X. Gu *et al.*, "Development, implementation, and characterization of a 64-element dual-polarized phased-array antenna module for 28-GHz high-speed data communications," *IEEE Trans. Microw. Theory Techn.*, vol. 67, no. 7, pp. 2975–2984, Jul. 2019.

[18] A. Nafe, M. Sayginer, K. Kibaroglu, and G. M. Rebeiz, "2 x 64 dual-polarized dual-beam single-aperture 28 GHz phased array with high cross-polarization rejection for 5G polarization MIMO," in *Proc. IEEE MTT-S Int. Microw. Symp.*, 2019, pp. 484–487.